2011 50th IEEE Conference on Decision and Control and
European Control Conference (CDC-ECC)
Orlando, FL, USA, December 12-15, 2011

Modeling CO_2 Recovery for Optimal Dynamic Operations

Ricardo Dunia, Gary T. Rochelle and S. Joe Qin

Abstract— **The development of amine scrubbing processes for coal and natural gas-fired power plants is essential to reduce CO_2 emissions. The design of tailor-made dynamic models to predict CO_2 capture in amine scrubbing processes is fundamental for optimal control operations. This paper presents the use of SIMPCA, a subspace system identification technique used to develop a dynamic empirical model for an LQG controller with integral action. Such a controller is made to attain optimal operating conditions for a CO_2 capture pilot plant. Reference signals are used in conjunction with the controller integral action to bring few process outputs towards their set-points. The results illustrate the importance of reliable model prediction in order to provide desirable closed loop response and appropriate CO_2 emission reduction.**

I. INTRODUCTION

The $\mathbf{CO_2}$ capture process with amine solvent based absorption and stripping is the most significant industrial method for the removal of carbon dioxide from coal and natural gas-fired power plants [1]. Dynamic models have been developed for the $\mathbf{CO_2}$ capture process [2] [3]. However, these models require the calculation of reaction kinetics and thermodynamic properties provided by specialized software not made for real time optimization. Therefore, the application of this type of models during process operations is limited because simulation convergence, time and computational resources are limited in industrial setups.

Data-driven empirical models, like subspace system identification, allow fast adjustment to process operations. Among empirical models, the subspace system identification algorithms have been well accepted in industry not only because of their simplicity and robustness, but also because they provide state space models that are very convenient for model based control [4] [5] [6]. This work implements a subspace system identification technique named SIMPCA [7] to develop dynamic empirical models for a multi-variable predictive controller with integral action. Such a controller model is based on data acquired for the $\mathbf{CO_2}$ capture pilot plant at the separation research center in Austin, Texas.

There is a diversity of predictive multi-variable controllers in the literature [8]. However, not all of them have been successfully implemented in industrial applications. This is because model maintenance and operator training play an important role in the durability of an advanced controller. Linear quadratic regulators with Kalman filters and integral action have been recently implemented in the control of solid oxide fuel cell gas turbine in hybrid power plant systems [9]. The results show that the LQR ensures better maintenance of the fuel cell stack voltage and temperature that improves fuel cell system durability. LQR has been also used in the control of rotor speed of wind turbines to reduce the drive-train fatigue damage and improve power regulation [10]. In this research work we use the LQR with a state estimator (LQG) and integral action to control a $\mathbf{CO_2}$ recovery process.

This paper is divided in the following manner: Section II introduces SIMPCA for empirical modeling of the $\mathbf{CO_2}$ capture pilot plant. The incorporation of integral action in the LQG controller is discussed in Section III. The $\mathbf{CO_2}$ capture process operations are discussed in Section IV, where the main manipulated variables and the number of states variables are determined. Model prediction is tested and the controller is implemented in Section V. The results illustrate the importance of accurate models for closed loop performance and stability. Section VI provides the conclusions and the future work.

II. SUBSPACE SYSTEM IDENTIFICATION

Several mathematical forms can be used to describe linear stochastic discrete state space models [11]. The one considered in this work is based on the following expressions,

$$\mathbf{x}(k+1) = \mathbf{A}\mathbf{x}(k) + \mathbf{B}\mathbf{u}(k) + \mathbf{w}(k) \quad (1)$$

$$\mathbf{y}(k) = \mathbf{C}\mathbf{x}(k) + \mathbf{D}\mathbf{u}(k) + \mathbf{v}(k) \quad (2)$$

where $\mathbf{x}(k)$ and $\mathbf{w}(\mathbf{k}) \in \Re^n$, $\mathbf{y}(k)$ and $\mathbf{v}(k) \in \Re^m$, and $\mathbf{u}(k) \in \Re^l$. The probabilistic distributions of $\mathbf{w}_k$ and $\mathbf{v}_k$ are used to determine the model estimation confidence against the output measurements accuracy. In this manner a Kalman filter is included in the linear state space formulation in order to correct the state dynamics based on the mismatch between the estimated outputs $\hat{\mathbf{y}}$ and the actual measurements $\mathbf{y}$ at each sample time k,

$$\hat{\mathbf{x}}(k+1) = \mathbf{A}\hat{\mathbf{x}}(k) + \mathbf{B}\mathbf{u}(k) + \mathbf{L}\left[\mathbf{y}(k) - \hat{\mathbf{y}}(k)\right] \quad (3)$$

$$\hat{\mathbf{y}}(k) = \mathbf{C}\hat{\mathbf{x}}(k) + \mathbf{D}\mathbf{u}(k) \quad (4)$$

where $\mathbf{L}$ is the steady state Kalman gain. Substitution of $\mathbf{e}(k) \equiv \mathbf{y}(k) - \hat{\mathbf{y}}(k)$ in Eqs.(3, 4) gives

$$\hat{\mathbf{x}}(k+1) = \mathbf{A}\hat{\mathbf{x}}(k) + \mathbf{B}\mathbf{u}(k) + \mathbf{L}\mathbf{e}(k) \quad (5)$$

$$\mathbf{y}(k) = \mathbf{C}\hat{\mathbf{x}}(k) + \mathbf{D}\mathbf{u}(k) + \mathbf{e}(k) \quad (6)$$

Ricardo Dunia and Gary T. Rochelle are with the Department of Chemical Engineering at The University of Texas, Austin, TX 78712, USA rdunia@che.utexas.edu, gtr@che.utexas.edu

S. Joe Qin is with the Department of Chemical Engineering and Material Sciences at the University of Southern California, CA 90089, USA sqin@usc.edu

978-1-61284-799-3/11/$26.00 ©2011 IEEE

The f future $\mathbf{y}$ vectors, starting from sample time k, can be appended in a composite vector $\mathbf{y}_f(k)$,

$$\mathbf{y}_f(k) = \begin{bmatrix} \mathbf{y}(k) \\ \mathbf{y}(k+1) \\ \vdots \\ \mathbf{y}(k+f-1) \end{bmatrix} \tag{7}$$

and the future time array adjoins N consecutive outcomes of future time vectors as columns, starting from $\mathbf{y}_f(k)$,

$$\mathbf{Y}_f = \begin{bmatrix} \mathbf{y}_f(k) & \mathbf{y}_f(k+1) & \cdots & \mathbf{y}_f(k+N-1) \end{bmatrix} \tag{8}$$

where $\mathbf{Y}_f \in \Re^{m.f \times N}$ is also known as the Hankel data matrix for future values of $\mathbf{y}$. In a similar way, Hankel data matrices are defined for past outcomes of $\mathbf{y}$,

$$\mathbf{Y}_p = \begin{bmatrix} \mathbf{y}_p(k) & \mathbf{y}_p(k+1) & \cdots & \mathbf{y}_p(k+N-1) \end{bmatrix} \tag{9}$$

where, $\mathbf{Y}_p \in \Re^{m.p \times N}$ and p represents the past horizon,

$$\mathbf{y}_p(k) = \begin{bmatrix} \mathbf{y}(k-p) \\ \mathbf{y}(k+1-p) \\ \vdots \\ \mathbf{y}(k-1) \end{bmatrix} \tag{10}$$

Hankel data matrices are also defined for the vectors $\hat{\mathbf{x}}$, $\mathbf{u}$, and $\mathbf{e}$ to obtain the following forward dynamic relation,

$$\mathbf{Y}_f(k) = \mathbf{\Gamma}_f \mathbf{X}(k) + \mathbf{H}_f \mathbf{U}_f(k) + \mathbf{G}_f \mathbf{E}_f(k) \tag{11}$$

where $\mathbf{\Gamma}_f$ is the extended observability matrix, and $\mathbf{H}_f$ and $\mathbf{G}_f$ are top triangular Toeplitz matrices, as are shown in the Appendix.

The SIM method applied in this work is known as SIM-PCA [7] and it first eliminates the effect of the state $\mathbf{X}(k)$ on $\mathbf{Y}_f(k)$ by pre-multiplying Eq.(11) with the orthogonal complement of $\mathbf{\Gamma}_f$ full column rank,

$$(\mathbf{\Gamma}_f^{\perp})^T \begin{bmatrix} \mathbf{I} & -\mathbf{H}_f \end{bmatrix} \begin{bmatrix} \mathbf{Y}_f \\ \mathbf{U}_f \end{bmatrix} (k) = (\mathbf{\Gamma}_f^{\perp})^T \mathbf{G}_f \mathbf{E}_f(k) \tag{12}$$

The elimination of $\mathbf{X}(k)$ by the projection on the orthogonal subspace of the $\mathbf{\Gamma}_f$ columns makes the mismatch between the actual and model outputs solely dependent of $\mathbf{E}_f$. For this reason a right side matrix multiplication is used to eliminate the effect of $\mathbf{E}_f$ in Eq.(12). The matrix $\mathbf{W}$, known as instrumental variable, is used to eliminate $\mathbf{E}_f$,

$$\mathcal{E}\{\mathbf{E}_f \mathbf{W}\} = \mathbf{0} \tag{13}$$

It has been shown that the matrix $\mathbf{Z}_p^T \equiv [\mathbf{Y}_p^T \quad \mathbf{U}_p^T]$ is a good choice for instrumental variable of $\mathbf{E}_f$ in the sense that [12],

$$\lim_{N \to \infty} \frac{1}{N} \mathbf{E}_f \mathbf{Z}_p^T = \mathbf{0} \tag{14}$$

Therefore, the expectation of the right hand side multiplication of Eq.(12) by $\mathbf{W} = \mathbf{Z}_p^T$ provides the following expression,

$$\lim_{N \to \infty} (\mathbf{\Gamma}_f^{\perp})^T \begin{bmatrix} \mathbf{I} & -\mathbf{H}_f \end{bmatrix} \mathbf{Z}_f \mathbf{Z}_p^T = \mathbf{0} \tag{15}$$

The application of PCA on an ergodic process, where past data is representative of the future behavior of the process, gives

$$\frac{1}{N} \mathbf{Z}_f(k) \mathbf{Z}_p^T(k) = \mathbf{P}\mathbf{T}(k) + \tilde{\mathbf{P}}\tilde{\mathbf{T}}(k) \tag{16}$$

which suggests from Eq.(15) that for $N \to \infty$,

$$\begin{bmatrix} \mathbf{\Gamma}_f^{\perp} \\ \mathbf{H}_f^T \mathbf{\Gamma}_f^{\perp} \end{bmatrix} = \tilde{\mathbf{P}}\mathbf{M} = \begin{bmatrix} \tilde{\mathbf{P}}_y \\ \tilde{\mathbf{P}}_u \end{bmatrix} \mathbf{M} \tag{17}$$

where $\mathbf{M}$ defines the non-trivial linear combination of the $\tilde{\mathbf{P}}$ columns. The matrix $\tilde{\mathbf{P}}$ is divided into the first $m.f$ rows, $\tilde{\mathbf{P}}_y$, and last $l.f$ rows, $\tilde{\mathbf{P}}_u$, which gives

$$\mathbf{\Gamma}_f = \tilde{\mathbf{P}}_y^{\perp} \qquad -\tilde{\mathbf{P}}_y^T \mathbf{H}_f = \tilde{\mathbf{P}}_u^T \tag{18}$$

Notice that the upper triangular matrix $\mathbf{H}_f$ has a defined column block structure as it is illustrated in the Appendix. For that reason, the following arrangement is made to define an upper triangular solution for $\mathbf{H}_f$,

$$\begin{aligned} -\tilde{\mathbf{P}}_y^T = \quad \mathbf{\Phi} \quad &\equiv \begin{bmatrix} \mathbf{\Phi}_1 & \cdots & \mathbf{\Phi}_f \end{bmatrix} \\ \tilde{\mathbf{P}}_u^T = \quad \mathbf{\Psi} \quad &\equiv \begin{bmatrix} \mathbf{\Psi}_1 & \cdots & \mathbf{\Psi}_f \end{bmatrix} \end{aligned}$$

where $\mathbf{\Phi}_i \in \Re^{(m.f-n) \times m}$ and $\mathbf{\Psi}_i \in \Re^{(m.f-n) \times l}$ are the i^{th} block column of $\mathbf{\Phi}$ and $\mathbf{\Psi}$, respectively. Given the structure of matrix $\mathbf{H}_f$ in the Appendix, only the first column block $\mathbf{H}_{f1}$ (defined by the first l columns) is necessary to determine the rest of the matrix. Therefore, the expression $\mathbf{\Phi}\mathbf{H}_f = \mathbf{\Psi}$ can be rearranged to,

$$\begin{bmatrix} \mathbf{\Phi}_1 & \mathbf{\Phi}_2 & \cdots & \mathbf{\Phi}_{f-1} & \mathbf{\Phi}_f \\ \mathbf{\Phi}_2 & \mathbf{\Phi}_3 & \cdots & \mathbf{\Phi}_f & \mathbf{0} \\ \vdots & \vdots & \ddots & \vdots & \vdots \\ \mathbf{\Phi}_f & \mathbf{0} & \cdots & \mathbf{0} & \mathbf{0} \end{bmatrix} \mathbf{H}_{f1} = \begin{bmatrix} \mathbf{\Psi}_1 \\ \mathbf{\Psi}_2 \\ \vdots \\ \mathbf{\Psi}_f \end{bmatrix} \tag{19}$$

where

$$\mathbf{H}_{f1} \equiv \begin{bmatrix} \mathbf{D} \\ \mathbf{CB} \\ \mathbf{CAB} \\ \vdots \\ \mathbf{CA^{f-2}B} \end{bmatrix} \tag{20}$$

A least square solution for $\mathbf{H}_{f1}$ is obtained from the over-determined Eq.(19). The lower triangular matrix $\mathbf{H}_f$ can be constructed from $\mathbf{H}_{f1}$.

The top m rows of matrices $\mathbf{\Gamma}_f^{\perp}$ and $\mathbf{H}_{f1}$ provide the estimation for the system matrices $\mathbf{C}$ and $\mathbf{D}$, respectively

$$\begin{aligned} \hat{\mathbf{C}} &= \mathbf{\Gamma}_f(1:m,:) \\ \hat{\mathbf{D}} &= \mathbf{H}_{f1}(1:m,:) \end{aligned}$$

The system matrices $\mathbf{A}$ and $\mathbf{B}$ are estimated by solving the least squares problems

$$\mathbf{\Gamma}_f(m+1:m.f,:) = \mathbf{\Gamma}_f(1:m.(f-1),:)\hat{\mathbf{A}} \tag{21}$$

and

$$\mathbf{H}_{f1}(m+1:m.f,:) = \mathbf{\Gamma}_f(1:m.(f-1),:)\hat{\mathbf{B}} \tag{22}$$

respectively. The matrix $\mathbf{G}_f$ is calculated from the QR decomposition of the matrix,

$$\begin{bmatrix} \mathbf{U}_p \\ \mathbf{Y}_p \\ \mathbf{U}_f \\ \mathbf{Y}_f \end{bmatrix} = \begin{bmatrix} \mathbf{R}_{11} & \mathbf{0} & \mathbf{0} & \mathbf{0} \\ \mathbf{R}_{21} & \mathbf{R}_{22} & \mathbf{0} & \mathbf{0} \\ \mathbf{R}_{31} & \mathbf{R}_{32} & \mathbf{R}_{33} & \mathbf{0} \\ \mathbf{R}_{41} & \mathbf{R}_{42} & \mathbf{R}_{43} & \mathbf{R}_{44} \end{bmatrix} \begin{bmatrix} \mathbf{Q}_1 \\ \mathbf{Q}_2 \\ \mathbf{Q}_3 \\ \mathbf{Q}_4 \end{bmatrix} \quad (23)$$

where only $\mathbf{R}_{44}$ and $\mathbf{Q}_4$ are required for the calculation of $\mathbf{G}_f$,

$$\mathbf{G}_f^* = \mathbf{R}_{44}\mathbf{Q}_4 \quad (24)$$

where $\mathbf{G}_f^* = \mathbf{G}_f\mathbf{F}$. From the structure of the matrix $\mathbf{G}_f$ given in the Appendix we obtain that the first m columns of $\mathbf{G}_f^*$ are given by

$$\mathbf{G}_{f1}^* \equiv \begin{bmatrix} \mathbf{F} \\ \mathbf{CLF} \\ \mathbf{CALF} \\ \vdots \\ \mathbf{CA^{f-2}LF} \end{bmatrix} \quad (25)$$

Therefore, $\hat{\mathbf{F}} = \mathbf{G}_{f1}^*(1:m,:)$ and

$$\mathbf{\Gamma}_f(1:m.(f-1),:)\hat{\mathbf{L}}\hat{\mathbf{F}} = \mathbf{G}_{f1}^*(m+1:m.f,:) \quad (26)$$

where the product $\hat{\mathbf{L}}\hat{\mathbf{F}}$ is obtained using least squares, and $\hat{\mathbf{F}}$ is in general nonsingular.

III. LQG WITH INTEGRAL ACTION

Process engineers dictate requirements for a set of process outputs to follow a list of reference variables, denoted by $\mathbf{r} \in \Re^s$. Such a condition introduces a list of integrators or additional states, denoted by $\mathbf{x}_I \in \Re^s$, that are necessary to determine the accumulated difference defined by $\mathbf{r} - \mathbf{I}_r\mathbf{y}$,

$$\mathbf{x}_I(k+1) = \mathbf{x}_I(k) + \mathbf{r}(k) - \mathbf{I}_r\mathbf{y}(k) \quad (27)$$

where rows of the matrix $\mathbf{I}_r \in \Re^{s\times m}$ define the set of outputs with assigned reference or set-point. The incorporation of these integrators determine the following steady state feasible condition,

$$\mathbf{r}^* = \mathbf{I}_r\mathbf{y}^* \quad (28)$$

where the subscripts $'*'$ denotes "steady state". A similar necessary condition for the original model to reach steady state is

$$\begin{bmatrix} \mathbf{A}-\mathbf{I} & \mathbf{B} \\ \mathbf{C} & \mathbf{D} \end{bmatrix} \begin{bmatrix} \hat{\mathbf{x}}^* \\ \mathbf{u}^* \end{bmatrix} = \begin{bmatrix} \mathbf{0} \\ \hat{\mathbf{y}}^* \end{bmatrix} \quad (29)$$

A control law that relates $\mathbf{u}$ to the states is necessary to determine an appropriate optimal steady state target. For convenience the LQR control law is here used,

$$\mathbf{u} = -\begin{bmatrix} \mathbf{K} & \mathbf{K}_I \end{bmatrix} \begin{bmatrix} \hat{\mathbf{x}} \\ \mathbf{x}_I \end{bmatrix}$$

which satisfies the steady state conditions,

$$\mathbf{u}^* = -\begin{bmatrix} \mathbf{K} & \mathbf{K}_I \end{bmatrix} \begin{bmatrix} \hat{\mathbf{x}}^* \\ {\mathbf{x}_I}^* \end{bmatrix} \quad (30)$$

The substitution of Eq.(30) in Eq.(29) provides the following equality constraint in the case of no system-model output mismatch, i.e. $\hat{\mathbf{y}}^* = \mathbf{y}^*$,

$$\begin{bmatrix} \mathbf{A}-\mathbf{I} & \mathbf{B} & \mathbf{0} & \mathbf{0} \\ \mathbf{C} & \mathbf{D} & \mathbf{0} & -\mathbf{I}_m \\ \mathbf{0} & \mathbf{0} & \mathbf{0} & \mathbf{I}_r \\ \mathbf{K} & \mathbf{I}_l & \mathbf{K}_I & \mathbf{0} \end{bmatrix} \begin{bmatrix} \hat{\mathbf{x}}^* \\ \mathbf{u}^* \\ {\mathbf{x}_I}^* \\ \hat{\mathbf{y}}^* \end{bmatrix} = \begin{bmatrix} \mathbf{0} \\ \mathbf{0} \\ \mathbf{r}^* \\ \mathbf{0} \end{bmatrix}$$

This last expression represents the equality constraint for the calculation of the optimal steady state target based on the following objective function,

$$\min_{\mathbf{u}^*} \mathbf{u}^{*T}\mathbf{R}\mathbf{u}^* + \chi^{*T}\mathbf{Q}\chi^* \quad (31)$$

where $\chi^{*T} \equiv \begin{bmatrix} \hat{\mathbf{x}}^{*T} & \mathbf{x}_I^{*T} \end{bmatrix}$, and the matrices $\mathbf{R}$ and $\mathbf{Q}$ weight the costs of the different inputs and states, respectively. Notice that these variables are defined in terms of their deviation from nominal conditions. When the degrees of freedom allow, inequality constraints can be also incorporated in the optimization scheme presented above,

$$\mathbf{u}_{min} \le \mathbf{u}^* \le \mathbf{u}_{max} \qquad \mathbf{y}_{min} \le \mathbf{y}^* \le \mathbf{y}_{max} \quad (32)$$

Such inequality constraints define the feasible region of operation. Notice that states are not included in the list of inequality constraints because they lack of physical meaning.

The LQR gain matrix $\mathbf{K}_c = [\mathbf{K} \quad \mathbf{K}_I]$ is calculated based on the minimization of the following objective function,

$$J = \sum_{k=0}^{h-1} \Delta\mathbf{u}^T(k)\mathbf{R}\Delta\mathbf{u}(k) + \Delta\chi^T(k)\mathbf{Q}\Delta\chi(k) \quad (33)$$

where $\Delta\mathbf{u}(0), \cdots, \Delta\mathbf{u}(h-1)$ are the adjustable variables. The operator Δ indicates deviation from the optimal steady state value, i.e. $\Delta\mathbf{u} \equiv \mathbf{u} - \mathbf{u}^*$. For convenience the matrices $\mathbf{R}$ and $\mathbf{Q}$ are considered identical to the ones used for the steady state case. The system matrices used for deviation variables are also identical to the ones defined for the original variables. Finally, the reference vector $\Delta\mathbf{r}$ is eliminated from the calculation of $\mathbf{K}_c$ as such inputs are not considered as manipulated variables. One way to discard the use of references as manipulated variables is by assigning large cost penalties in the objective function, J.

The controller design procedure described above provides the following controller structure,

$$\begin{aligned} \Delta\chi(k+1) &= \mathbf{\Lambda}\Delta\chi(k) + \mathbf{\Omega}\begin{bmatrix} \Delta\mathbf{y} \\ \Delta\mathbf{r} \end{bmatrix}(k) \\ \Delta\mathbf{u}(k) &= -\mathbf{K}_c\Delta\chi(k) \end{aligned}$$

where the matrices $\mathbf{\Lambda}$ and $\mathbf{\Omega}$ are given in the Appendix. Notice that such a controller structure includes the state estimator as well as the controller integrators. Figure 1 illustrates how this controller exchanges data with the process sensors as well as to the steady state optimizer to determine the optimal control action, $\mathbf{u}(k)$. The $\mathbf{G}_f$ block is used to smooth the steady state reference and avoid drastic changes in the calculation of the controller action, $\mathbf{u}$.

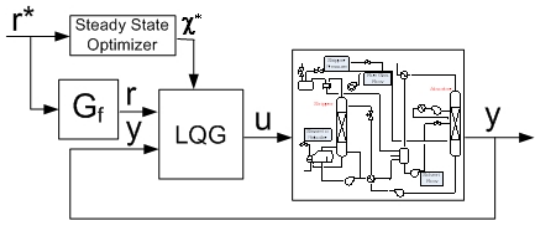

Fig. 1. Block diagram of LQG Controller with Integral Action.

IV. MODELING CO_2 RECOVERY PROCESS

The CO_2 capture plant consists of absorbtion and stripping columns. The absorber receives typical coal fired flue gas containing 10 to 12 % CO_2 at 40 to 60 ^oC and at atmospheric pressure. Figure 2 illustrates the absorption column on the right. Purified gas with low CO_2 leaves the top of the absorber column to the atmosphere. The stripper column removes the CO_2 from the liquid stream by increasing the temperature to about 120^oC at the bottom. Steam is used at the reboiler to heat the aqueous solution.

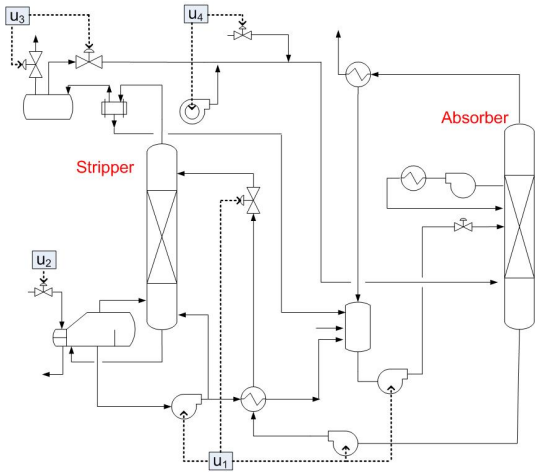

Fig. 2. CO_2 capture pilot process flow diagram. The purified gas and captured CO_2 are mixed and recycled to the absorber. The four main input variables are highlighted in the diagram. These are the solvent flow (u_1), reboiler steam flow (u_2), the stripper pressure (u_3) and the flue gas flow (u_4).

There are four main input variables that define the operating conditions of this pilot plant. These variables have been highlighted in Figure 2 and are manipulated or considered as input disturbances to the process. These are:

- *Solvent flow circulation*: the solvent flow rate can be adjusted by variable speed pumps throughout the whole plant while maintaining liquid holdups.
- *Flue gas load*: the gas load is a function of the amount of flue gas that needs to be processed from the power plant exhaust stack. Such a flow depends in many occasions of the amount of electric power generated.
- *Reboiler steam flow*: the steam flow regulates the temperature in the stripper bottom and the amount of CO_2 removed from the solvent. High steam consumption is detrimental to the power plant efficiency, as in average 30% of low pressure steam available in the power plant is consumed in the reboiler.
- *Stripper pressure*: the stripper pressure is regulated by the amount of gas removed from the rich loading stream, which is also a function of the reboiler steam flow.

Process variables are intrinsically correlated and that a supervisory control level can be implemented to adjust plant operations. Therefore, only few state variables representing the dynamics of the process holdups and delays should be necessary to define the process transients. This data compression to just a few dynamic states demonstrates the advantage of subspace system identification methods to describe plant modes of operation.

SIMPCA is used to develop the dynamic model for the CO_2 capture plant. The optimal number of states n is determined by the Akaike Information Criterion index [13]. The data collected from the plant consists of 69 normalized output measurements. The inputs were compressed into the four independent decision variables described above. Table I illustrates the AIC index for 310 samples taken every 15 seconds, where ten samples were used for the past and future horizons. Base on such a criterion, the optimum number of states that represents the process dynamics is 6, where $AIC(6) = 11.2\ 10^3$.

TABLE I
AIC INDEX FOR THE DIFFERENT NUMBER OF STATES.

n	4	5	6	7	8
$AIC.10^{-3}$	33.8	21.5	11.2	13.6	16.8

The fact that SIMPCA models are empirical prevents each state to represent a material/energy holdup, as it would have been the case of first principle models. Nevertheless, a state profile can well be a linear combination of the process holdup dynamic responses.

V. MODEL PREDICTION AND OPTIMAL CONTROL

A. Model Prediction

Model prediction is of significant importance in model based control applications. It consists of the calculation of future process outputs based on current and previous input-output measurements. A Kalman filter is used to estimate initial conditions for output prediction. After such an initial state is estimated, the model prediction rescinds of the filter term because future process measurements are not available to correct the model dynamics. Therefore, the following procedure is used to calculate an h step ahead prediction profile:

1 Allow an initial number of samples κ for a reliable estimation of the initial states $\mathbf{x}(\kappa)$ using Eqs.(1, 2). Such expressions include the Kalman filter in order to make the adequate correction in the model dynamics.
2 Given $\mathbf{x}(\kappa)$ and $\mathbf{u}(\kappa : \kappa+h)$ from the historian calculate $\mathbf{x}(\kappa+1 : \kappa+h)$ using Eq.(1) but without the filter term.

3 Using the last state and input vectors of the prediction window $\mathbf{x}(\kappa+h)$ and $\mathbf{u}(\kappa+h)$ determine $\mathbf{y}(\kappa+h)$ from Eq.(2).
4 Calculate $\hat{\mathbf{x}}(\kappa+1)$ using Eq.(1) and the actual output vector $\mathbf{y}(\kappa)$ from the sensor measurements. Repeat the procedure starting from step 2.

Notice that the vector $\mathbf{y}(\kappa+h)$ represents the output prediction h samples in the future. Figure 3 illustrates the effect of the prediction horizon in the the stripper bottom temperature estimation. Only the last element of the prediction window is shown for each plot line. After this output is estimated h samples in the future, the prediction window steps one sample forward, and new measured outputs are made available for the Kalman filter to estimate new initial conditions. This procedure is repeated until all the data collected for testing is considered.

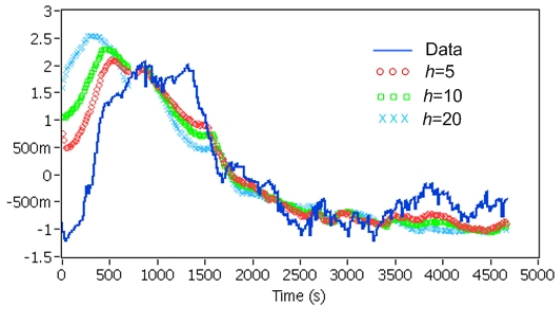

Fig. 3. Effect of the prediction horizon in the stripper bottom temperature estimation. The larger the prediction horizon the less accurate is the prediction.

Model prediction precision determines the accuracy of the controller gain calculations, as these are based of the model system matrices. Next section illustrates the use of model prediction in optimal control operations for the $\mathbf{CO_2}$ recovery process.

B. Optimal $\mathbf{CO_2}$ Recovery Under Transient Operations

The model identified in Section IV is used to develop a Linear Quadratic Gaussian controller (LQG) with integral action. The integral action is achieved by augmenting the state vector with integrators and providing the respective reference profiles for the controlled variables, CVs. Therefore, the controller will maintain zero offset for the chosen CVs even in the presence of process-model mismatch.

The $\mathbf{CO_2}$ concentration at the top of the absorber (y_8) and the rich $\mathbf{CO_2}$ gas flow at the top of the stripper (y_{39}) were chosen as CVs. All inputs, with the exception of the flue gas flow disturbance, are adjusted by the controller to achieve optimal operating responses. The cost weight matrix $\mathbf{R}$ has been designed based on the different manipulated variables costs. In a similar manner, state deviation from nominal conditions are also penalized based on the following state-output weight conversion,

$$\mathbf{Q} = \mathbf{C}^T \mathbf{Q}_y \mathbf{C} \tag{34}$$

where $\mathbf{Q}_y$ is the weight cost matrix for the output deviation vector.

Figure 4 illustrates the closed loop time response to $\mathbf{r}^* = [-1 \quad 1]^T$. The CVs reach their respective reference values within 1500 s (100 samples), while the MVs show a smooth trajectory towards their desirable steady states. It is important to emphasize that the controller internal model considered in these responses is identical to the actual system.

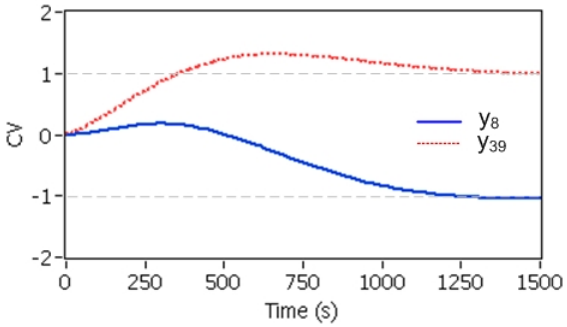

(a) CVs are the $\mathbf{CO_2}$ concentration at the top of the absorber (y_8) and the rich $\mathbf{CO_2}$ gas flow at the top of the stripper (y_{39})

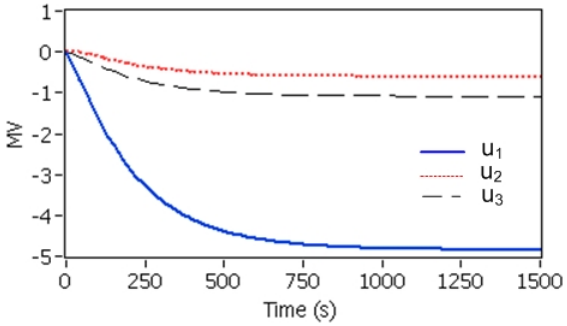

(b) MVs are the solvent flow (u_1), reboiler steam flow (u_2) and stripper pressure (u_3)

Fig. 4. Closed loop time response to $\mathbf{r}^* = [-1 \quad 1]^T$ using LQG with integral action.

There are several studies that determine the detrimental effect of process-model mismatch [14] [15]. In the case of the LQR with integral action, the response can be deteriorated to the point that closed loop responses can become unstable when this mismatch is significant. To illustrate the effect of process-model mismatch, the $\mathbf{A}$ matrix of the process, denoted by $\mathbf{A}_{sys}$ is modified based on the following expression:

$$\mathbf{A}_{sys} = \mathbf{A} + \alpha\mathcal{A}$$

where $\mathcal{A}$ represents the mismatch matrix and $0 \leq \alpha \leq 1$ determines the magnitude of the mismatch. Figure 5 illustrates the effect of the mismatch in the phase diagram defined by the CVs. Notice that for $\alpha = 1$ the response becomes oscillatory and unstable. In such a case the integral action intends to bring the system towards the $[-1 \quad 1]$ target point but the process-model discrepancy prevents the controller to provide a stable closed loop response.

VI. CONCLUSIONS AND FUTURE WORK

The Subspace Identification Method with Principal Component Analysis (SIMPCA) is successfully used to develop a dynamic empirical model for the $\mathbf{CO_2}$ recovery pilot

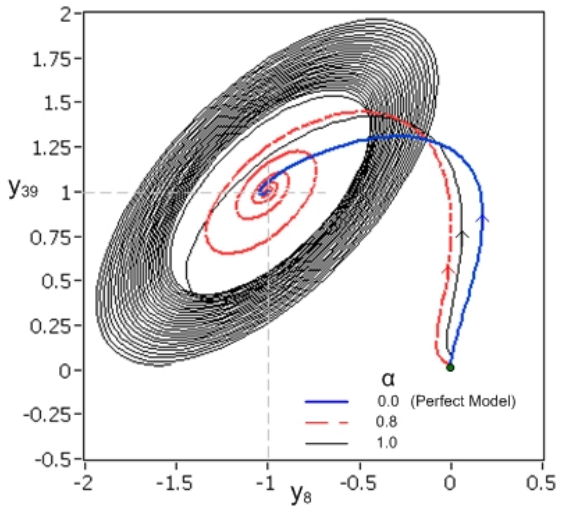

Fig. 5. Effect of process-model mismatch in the CVs phase diagram.

plant at the separation research center in Austin, Texas. This model predicts the dynamic response of more than sixty outputs with only six dynamic states. Four main decision variables are used to bring the plant from one operating condition to another. A multi-variable LQG controller is here developed based on the SIMPCA model in order to assist the operators in stabilizing the plant in an optimal manner around desirable operating conditions. The results show that LQG is well capable of bringing the plant to optimal steady state conditions in cases where the controller model provides a reliable prediction of the system outputs. Model Predictive Control (MPC) will be incorporated as future work in the controller structure to account for potential constraints during significant power consumption swinging.

ACKNOWLEDGMENTS

The authors gratefully acknowledge Frank Seibert and Micah Perry for providing the data and operational insight used to develop the dynamic model.

APPENDIX

The extended observability matrix $\mathbf{\Gamma}_f$ is given by:

$$\mathbf{\Gamma}_f = \begin{bmatrix} \mathbf{C} \\ \mathbf{CA} \\ \vdots \\ \mathbf{CA^{f-1}} \end{bmatrix} \in \Re^{mf \times n}$$

while $\mathbf{H}_f$ and $\mathbf{G}_f$ are lower triangular Toeplitz matrices,

$$\mathbf{H}_f = \begin{bmatrix} \mathbf{D} & \mathbf{0} & \cdots & \mathbf{0} \\ \mathbf{CB} & \mathbf{D} & \cdots & \mathbf{0} \\ \vdots & \vdots & \ddots & \vdots \\ \mathbf{CA}^{f-2}\mathbf{B} & \mathbf{CA}^{f-3}\mathbf{B} & \cdots & \mathbf{D} \end{bmatrix} \in \Re^{mf \times lf}$$

$$\mathbf{G}_f = \begin{bmatrix} \mathbf{I} & \mathbf{0} & \cdots & \mathbf{0} \\ \mathbf{CK} & \mathbf{I} & \cdots & \mathbf{0} \\ \vdots & \vdots & \ddots & \vdots \\ \mathbf{CA}^{f-2}\mathbf{L} & \mathbf{CA}^{f-3}\mathbf{L} & \cdots & \mathbf{I} \end{bmatrix} \in \Re^{mf \times mf}$$

and determine the effect of the inputs and estimation errors on the state dynamics. For the LQG controller structure, the following matrices are considered:

$$\mathbf{\Lambda} = \begin{bmatrix} \mathbf{A - LC - BK + LDK} & \mathbf{LDK}_I \mathbf{- BK}_I \\ \mathbf{I}_r\mathbf{CBK - I}_r\mathbf{C} & \mathbf{I + I}_r\mathbf{CBK}_I \end{bmatrix}$$

$$\mathbf{\Omega} = \begin{bmatrix} \mathbf{L} & \mathbf{0} \\ \mathbf{0} & \mathbf{I} \end{bmatrix}$$

Notice that the state estimator as well as the controller integrators are already imbedded in such matrices.

REFERENCES

[1] J. M. Plaza, D. Van Wagener, G. T. Rochelle, Modeling CO2 Capture with Aqueous Monoethanolamine, in: Gale, J and Herzog, H and Braitsch, J (Ed.), GREENHOUSE GAS CONTROL TECHNOLOGIES 9, Vol. 1 of Energy Procedia, 2009, pp. 1171–1178, 9th International Conference on Greenhouse Gas Control Technologies, Washington, DC, NOV 16-20, 2008. doi:10.1016/j.egypro.2009.01.154.

[2] S. Ziaii, G. T. Rochelle, T. F. Edgar, Dynamic Modeling to Minimize Energy Use for CO2 Capture in Power Plants by Aqueous Monoethanolamine, INDUSTRIAL & ENGINEERING CHEMISTRY RESEARCH 48 (13) (2009) 6105–6111. doi:10.1021/ie801385q.

[3] H. M. Kvamsdal, J. P. Jakobsen, K. A. Hoff, Dynamic modeling and simulation of a CO2 absorber column for post-combustion CO2 capture, CHEMICAL ENGINEERING AND PROCESSING 48 (1) (2009) 135–144. doi:10.1016/j.cep.2008.03.002.

[4] B. Wahlberg, M. Jansson, T. Matsko, M. A. Molander, Experiences from subspace system identification - Comments from process industry users and researchers, Vol. 364 of LECTURE NOTES IN CONTROL AND INFORMATION SCIENCES, 2007, pp. 315–327.

[5] W. Favoreel, B. De Moor, P. Van Overschee, Subspace state space system identification for industrial processes, JOURNAL OF PROCESS CONTROL 10 (2-3) (2000) 149–155, 5th IFAC Symposium on Dynamics and Control of Process Systems (DYCPOPS 5), CORFU, GREECE, JUN 08-10, 1998.

[6] M. Basseville, M. Abdelghani, A. Benveniste, Subspace-based fault detection algorithms for vibration monitoring, AUTOMATICA 36 (1) (2000) 101–109.

[7] J. Wang, S. Qin, A new subspace identification approach based on principal component analysis, JOURNAL OF PROCESS CONTROL 12 (8) (2002) 841–855.

[8] Y. Zhu, F. Butoyi, Case studies on closed-loop identification for MPC, CONTROL ENGINEERING PRACTICE 10 (4) (2002) 403–417.

[9] F. Mueller, F. Jabbari, J. Brouwer, S. T. Junker, H. Ghezel-Ayagh, Linear Quadratic Regulator for a Bottoming Solid Oxide Fuel Cell Gas Turbine Hybrid System, JOURNAL OF DYNAMIC SYSTEMS MEASUREMENT AND CONTROL-TRANSACTIONS OF THE ASME 131 (5). doi:10.1115/1.3155007.

[10] A. Kumar, K. Stol, Simulating feedback linearization control of wind turbines using high-order models, WIND ENERGY 13 (5) (2010) 419–432. doi:10.1002/we.363.

[11] S. J. Qin, An overview of subspace identification, COMPUTERS & CHEMICAL ENGINEERING 30 (10-12) (2006) 1502–1513, 7th International Conference on Chemical Process Control (CPC 7), Lake Louise, CANADA, JAN 08-13, 2006. doi:10.1016/j.compchemeng.2006.05.045.

[12] M. VERHAEGEN, Identification of the Deterministic Part of MIMO State-Space Models given in Innovations form from Input-Output Data, AUTOMATICA 30 (1) (1994) 61–74.

[13] M. Matsubara, Y. Usui, S. Sugimoto, System identification and order determination using canonical-forms, INTERNATIONAL JOURNAL OF INNOVATIVE COMPUTING INFORMATION AND CONTROL 1 (3) (2005) 527–545, Annual International Symposium on Stochastic Systems Theory and Its Applications (SSS), Saitama, JAPAN, NOV 03-04, 2004.

[14] M. Bruwer, J. MacGregor, Robust multi-variable identification: Optimal experimental design with constraints , JOURNAL OF PROCESS CONTROL 16 (6) (2006) 581–600.

[15] J. Hahn, M. Monnigmann, W. Marquardt, A method for robustness analysis of controlled nonlinear systems, CHEMICAL ENGINEERING SCIENCE 59 (20) (2004) 4325–4338. doi:10.1016/j.ces.2004.06.026.